Electronic Supplementary Material (ESI) for Journal of Materials Chemistry A
This journal is (c) The Royal Society of Chemistry 2013

Electronic Supplementary Information (ESI)

Composite structure and properties of Mn_3O_4/graphene oxide and Mn_3O_4/graphene

Lu Wang,[ab] Yuhong Li,[a] Zhida Han,[a] Lin Chen,[b] Bin Qian,[a] Xuefan Jiang,[a] João Pinto[c] and Gang Yang*[ac]

[a] Jiangsu Laboratory of Advanced Functional Material, Changshu Institute of Technology, Changshu 215500, China

[b] School of Material Science and Engineering, Jiangsu University of Science and Technology, Zhenjiang 212003, China

[c] Department of Physics & I3N, University of Aveiro, Campus Universitário de Santiago, 3810-193 Aveiro, Portugal

* Corresponding Authors. E-mail: gyang@cslg.edu.cn

Electronic Supplementary Material (ESI) for Journal of Materials Chemistry A
This journal is (c) The Royal Society of Chemistry 2013

Table S1. Summary of electrochemical measurements reported in recent papers for Mn_3O_4/RGO (or GO) nanocomposite as electrode material for ECs.

Preparation method	Nature of Mn_3O_4	Current collector	Electrolyte	Potential window	Measurement Protocol[a]	Maximum specific capacitance ($F\ g^{-1}$)	Capacitance retention after cycle test	Ref[b] (year)
Precipitation from MnO_2 organosol	Mn_3O_4/ RGO, Powder	Plantinum foil	1 M Na_2SO_4	-0.2-0.8V	CV (v =5 mV s^{-1})	175	-	27 (2010)
			6 M KOH	-0.5-0.5V		256		
Hydrothermal	Mn_3O_4/ RGO, Powder	Nickel grid	2 M KOH	-0.5-0.4V	Cp (i = 1 A g^{-1})	236.7	93.68 % after 1000 cycles	24 (2012)
Hydrothermal	Mn_3O_4/ RGO, Powder	Ni foam	1 M Na_2SO_4	-0.3-0.7V	CV (v =5 mV s^{-1})	114	100 % after 10,000 cycles	25 (2012)
				-0.1-0.7V	Cp (i = 0.5 A g^{-1})	121		
Hydrothermal	Mn_3O_4/ RGO, Powder	A stainless steel foil	1 M Na_2SO_4	-0.1-0.8V	Cp (i = 1 A g^{-1})	130	95 % after 1000 cycles	26 (2012)
Ultrasonic assisted	Mn_3O_4/ GO, Powder	Graphite sheet	1 M Na_2SO_4	0-1V	Cp (i = 2 A g^{-1})	247.7	124.6 % after 2000 cycles	This work
					Cp (i = 10 A g^{-1})	232.6	98.1 % after 9000 cycles	

[a] CV = Cyclic Voltammetry, Cp = Chronopotentiometry, v = Scan rate, i = Current density.
[b] References 24–27 can be found in the Notes and References section of the main article.

Electronic Supplementary Material (ESI) for Journal of Materials Chemistry A
This journal is (c) The Royal Society of Chemistry 2013

Table S2. The C 1s and O 1s binding energy values of GO and RGO

	C1s (eV)				O1s (eV)		
Sample	C-C	C-O	C=O	O-C=O	C-O	C=O	O-Mn
GO	284.6	286.7	287.7	288.4	531.2	532.5	-
Mn_3O_4/GO	284.6	286.2	287.9	289.1	531.1	532.4	529.5
Mn_3O_4/RGO	284.6	286.0	287.8	289.0	531.2	532.7	529.7

Preparation

Synthesis of graphite oxide (GiO). 100 ml of concentrated H_2SO_4 (98 %) were added slowly into the mixture of 2.0 g of KNO_3 and 4.0 g of natural graphite (300 mesh) at -15 ^oC. The mixture was stirred for 1 h before slow addition of 15 g $KMnO_4$ in an hour. Then, the mixture was heated to 38 ^oC and stirred for 3 hours. Subsequently, 180 ml of water was dropwise added under vigorous stirring, causing a quick rise in temperature to near 100 ^oC. The slurry was stirred at this temperature for another 3 hours. Afterwards, 20 ml of H_2O_2 solution (30 wt%) and 110 ml of water were added sequentially to dissolve insoluble manganese species. The resulting graphite oxide suspension was filtrated and washed using 800 ml dilute HCl (3%) solution. After dispersing the collected precipitate into 1200 ml boiling water, the solution was centrifuged and washed repeatedly with boiling water until the pH of the filtrate was neutral. The colloidal GiO was obtained and dried under vacuum at 80 ^oC for 3 days. The resulting product was ground into powder (100 mesh).

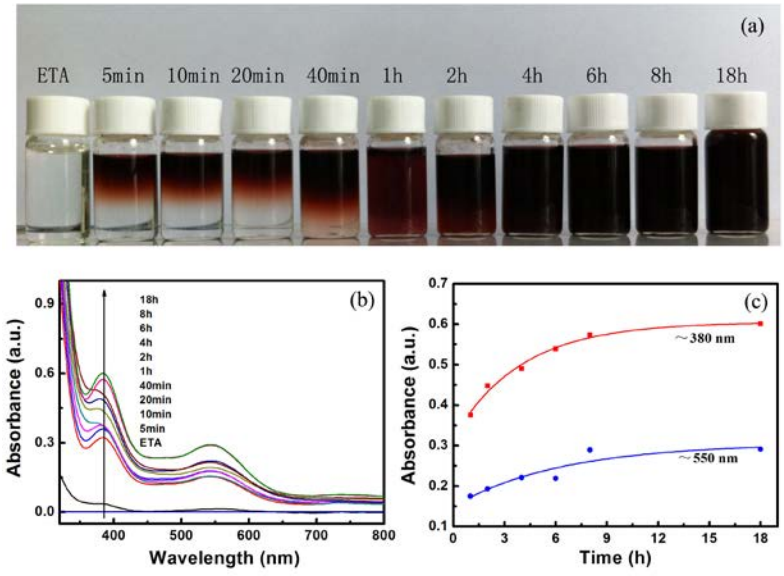

Fig. S1 (a) Digital photographs of Mn-complex collected at different ultrasonic time intervals, and (b) UV-vis spectra of these samples; (c) plot of UV-vis peak intensity of Mn-complex samples as a function of ultrasonic time.

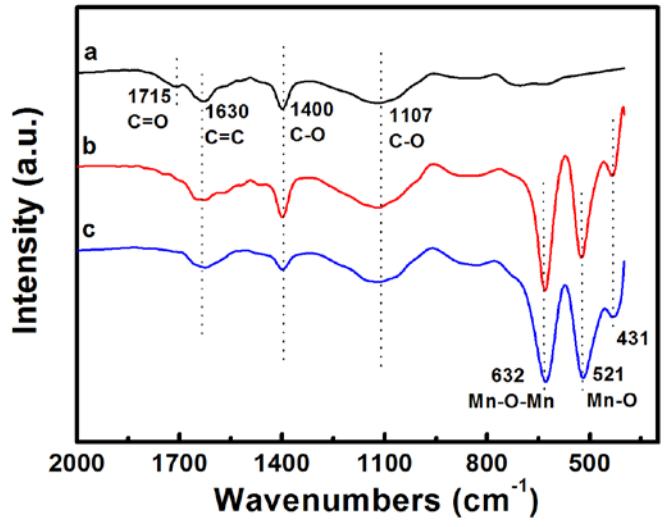

Fig. S2 FTIR spectrum: (a) GO, (b) Mn_3O_4/GO and (c) Mn_3O_4/RGO nanocomposites.

In order to further differentiate the structure of Mn_3O_4 component in the composites, FTIR analyses of GO, Mn_3O_4/GO and Mn_3O_4/RGO were performed and the corresponding spectra are shown in Figure S2. In the spectrum of GO, the absorption band at 1715 cm^{-1} is attributed to the C=O of carbonyl and carboxyl groups. While the absorption band at 1630 cm^{-1} is assigned to the vibration of the aromatic C=C. Moreover, the C–O stretching band at 1107 cm^{-1} can also be observed. In contrast to GO, the typical C=O absorption bands at 1715 cm^{-1} of Mn_3O_4/GO almost disappear, suggesting that the formation of the weak interaction in Mn--O–C, which leading to the emerging of the enhanced C–O instead of weak C=O. Moreover, the intensity of the absorption peaks related to the oxidized groups decreased slightly in the FTIR spectra of the Mn_3O_4/RGO composites prepared from GO relative to those in the spectrum of pure GO, indicating that reduction of GO and restoration of the conjugated aromatic system has occurred in the composite.[2]

In addition, two new peaks located at 521 and 632 cm^{-1} occurred in the spectra of Mn_3O_4/GO and Mn_3O_4/RGO, which can be associated with the coupling modes between the Mn-O stretching modes of tetrahedral and octahedral sites.[1] The absorption peak at 431 cm^{-1} is attributed to the band stretching modes of the octahedral sites, and displacement of the Mn^{2+} ions in the tetrahedral sites is negligible.[3]

Electronic Supplementary Material (ESI) for Journal of Materials Chemistry A
This journal is (c) The Royal Society of Chemistry 2013

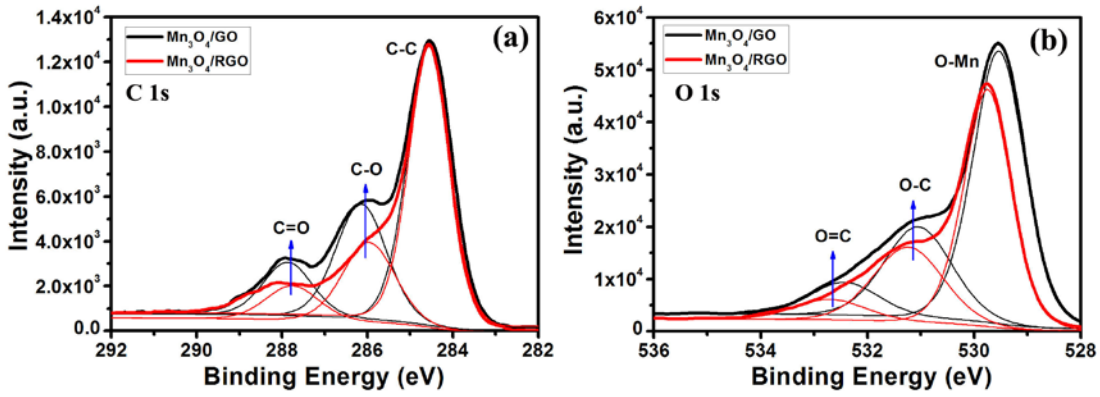

Fig. S3 The comparison of the peak intensities of (a) XPS C 1s spectra of Mn_3O_4/GO and Mn_3O_4/RGO and (b) O 1s spectra of Mn_3O_4/GO and Mn_3O_4/RGO.

Electronic Supplementary Material (ESI) for Journal of Materials Chemistry A
This journal is (c) The Royal Society of Chemistry 2013

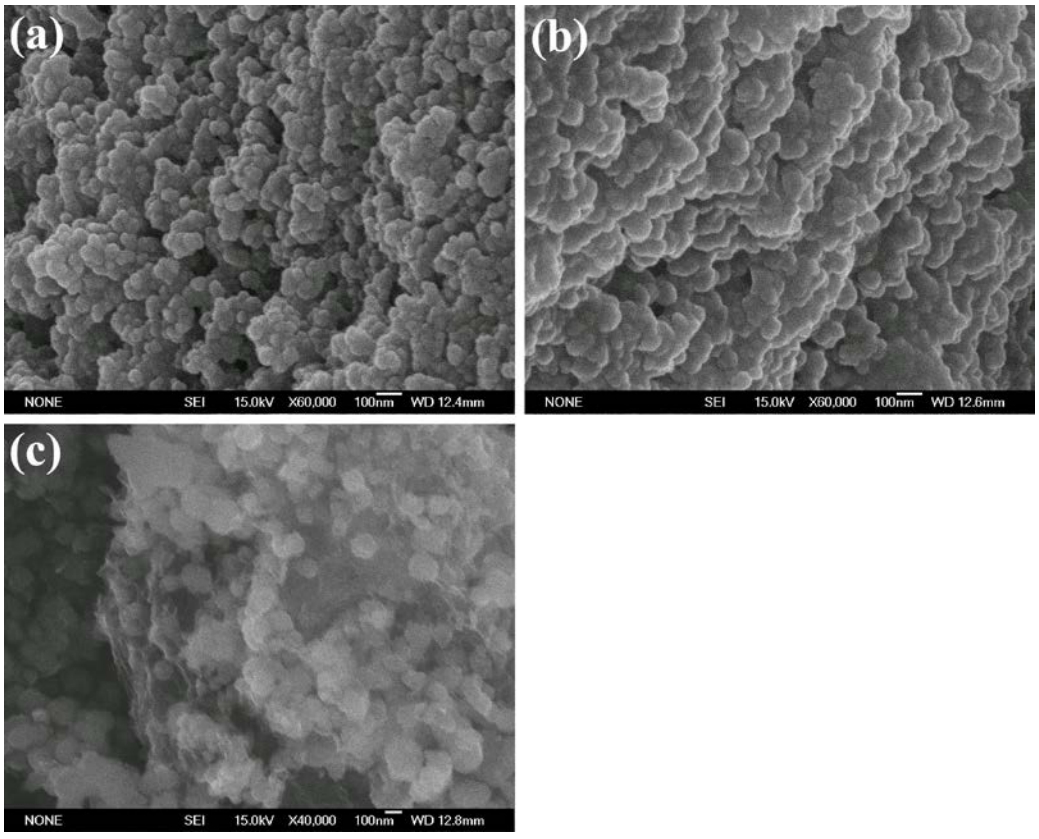

Fig. S4 SEM images of the samples (a) Mn_3O_4, (b) Mn_3O_4/GO and (c) Mn_3O_4/RGO nanocomposites.

Electronic Supplementary Material (ESI) for Journal of Materials Chemistry A
This journal is (c) The Royal Society of Chemistry 2013

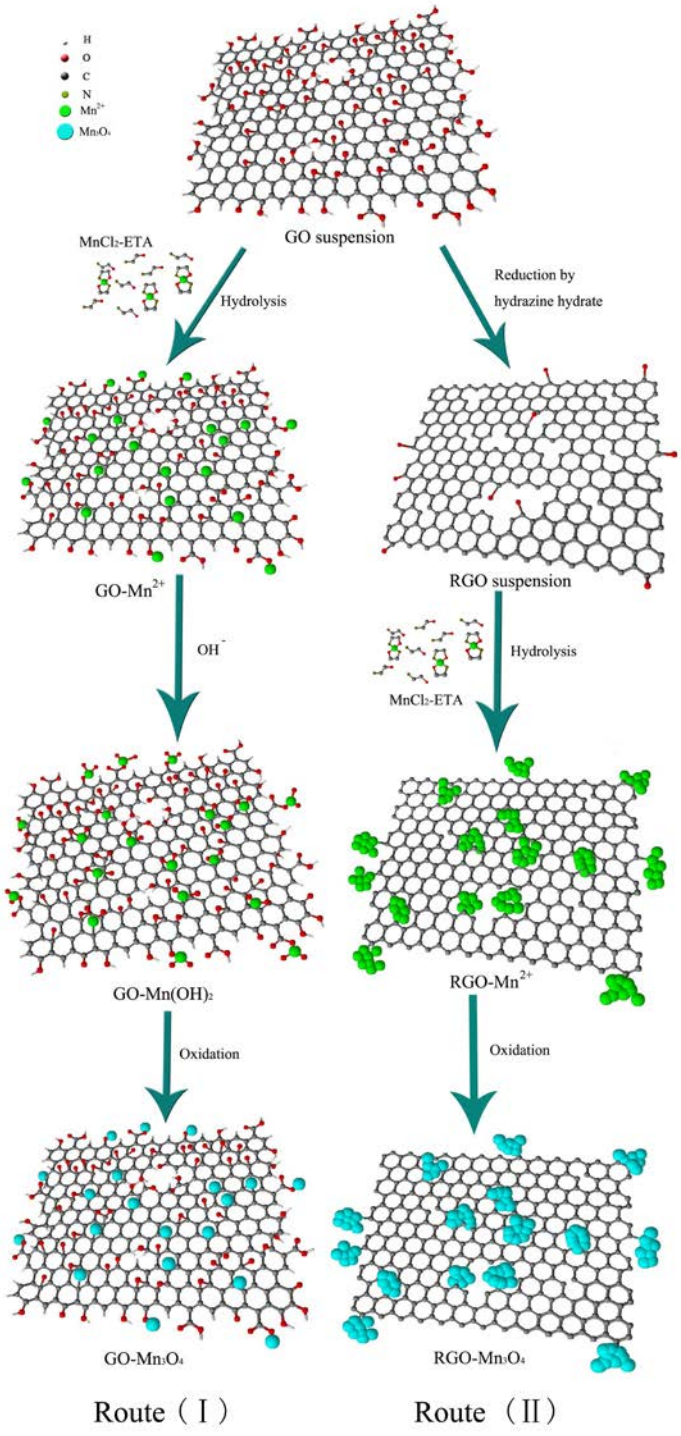

Scheme S1 The formation mechanism for Mn_3O_4 nanoparticle on the surface of GOs and RGOs.

Electronic Supplementary Material (ESI) for Journal of Materials Chemistry A
This journal is (c) The Royal Society of Chemistry 2013

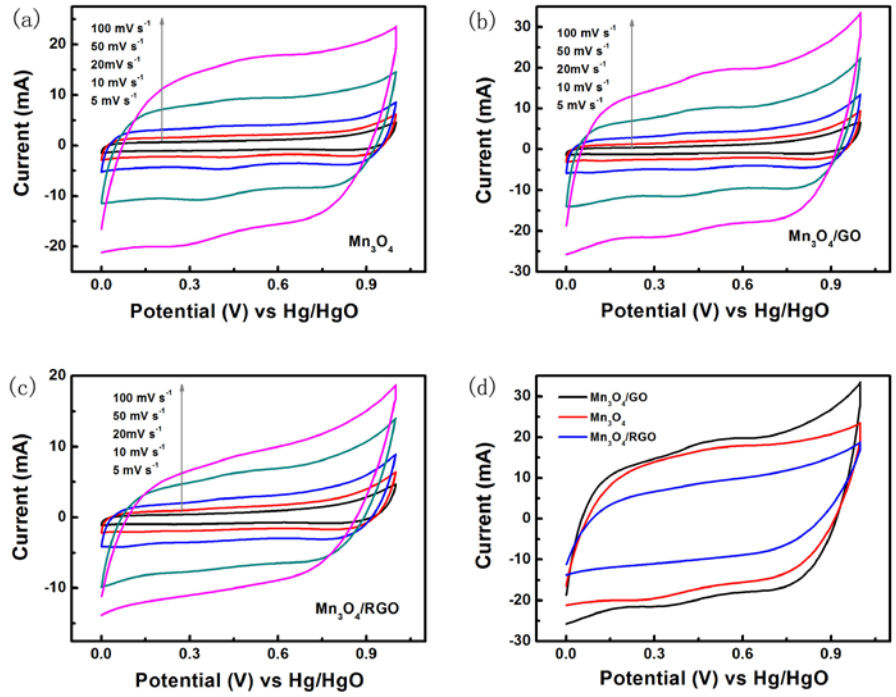

Fig. S5 (a-c) CV curves of bare Mn_3O_4, Mn_3O_4/GO nanocomposite and Mn_3O_4/RGO nanocomposite at different scan rates of 5, 10, 20, 50 and 100 mV s^{-1}, (d) CV curves of bare Mn_3O_4, Mn_3O_4/GO and Mn_3O_4/RGO nanocomposites at 100 mV s^{-1}.

Electronic Supplementary Material (ESI) for Journal of Materials Chemistry A
This journal is (c) The Royal Society of Chemistry 2013

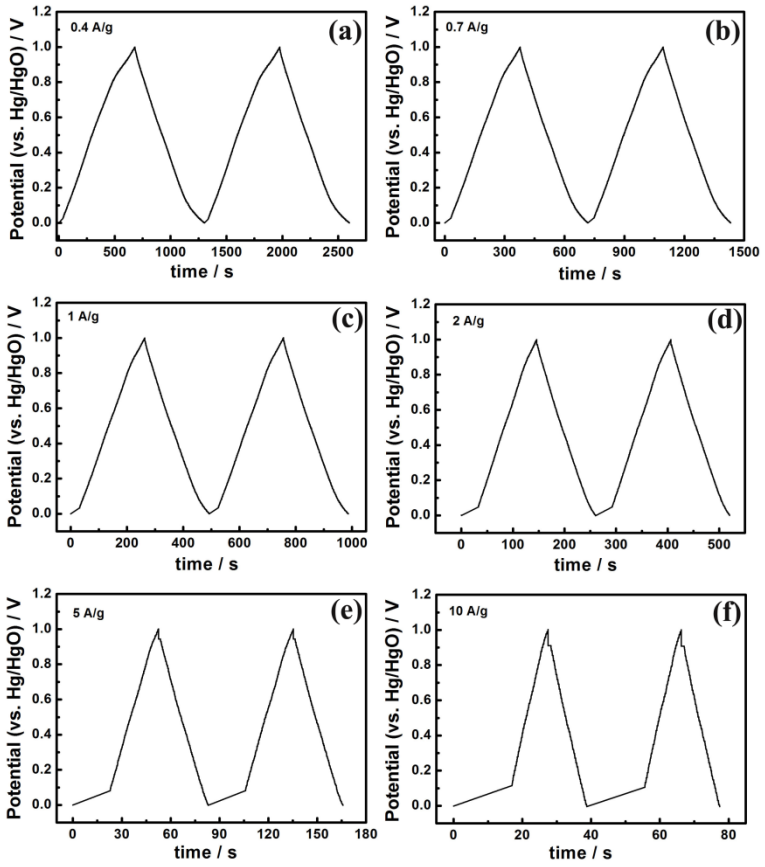

Fig. S6 Galvanostatic charge/discharge curves of Mn_3O_4/GO nanocomposite at different current densities from 0.4 to 10 A g^{-1}.

Electronic Supplementary Material (ESI) for Journal of Materials Chemistry A
This journal is (c) The Royal Society of Chemistry 2013

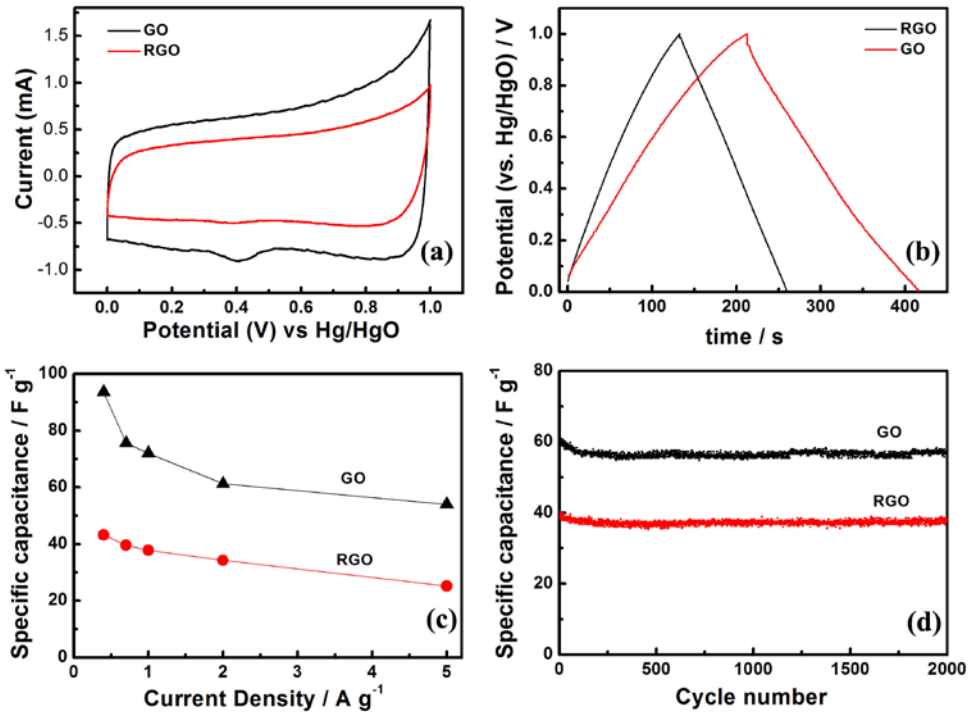

Fig. S7 (a) CV curves of GO and RGO at the scan rates of 10 mV s^{-1}, (b) galvanostatic charge/discharge curves of GO and RGO at 0.4 A g^{-1}, (c) rate performance of GO and RGO at different current densities from 0.4 A g^{-1} to 5 A g^{-1}, and (d) long cycle life of GO and RGO at 2 A g^{-1}.

The supercapacitor performance of GO and RGO are shown in Figure S7. In Figure S7.a, the CV curve of RGO shows a typical rectangular shape, implying pure electric double layer capacitive behavior and GO shows a box-like shape indicating the presence of pseudo-capacitance, which are agree with the phenomena in the previous publication.[49] The different capacitive behavior of GO and RGO is further confirmed by galvanostatic charge/discharge curves, as shown in Figure S7.b. The voltage-time curve of RGO shows an ideal linear shape, while a little deviation from the line can be observed for GO. The

deviations of the CV and V-t curves are related to the quick Faradaic reactions at the electrode interfaces (e. g. >C–OH <=> >C=O + H^+ + e^-, etc.). Abundant oxygen-containing functional groups of GO provide a large additional pseudo-capacitance, giving GO a higher capacitance than RGO. As shown in Figure S7.c, GO exhibits better capacity and rate performance than RGO, for example, the specific capacitance value of GO reach 93.6 F g^{-1} at 0.4 A g^{-1}, 54 F g^{-1} at 5 A g^{-1}, much higher than 43.2 F g^{-1} at 0.4 A g^{-1} and 25.2 F g^{-1} at 5 A g^{-1} of RGO. Figure S7.d shows the cycle stability of GO and RGO at current density of 2 A g^{-1}, both of them exhibit the excellent cycle stability, besides the much higher capacitance of GO than that of RGO. Based on the above experimental data, the abundant O-containing functional groups in GO structure are helpful for accumulating of charge, leading to higher capacitance of Mn_3O_4/GO than that of Mn_3O_4/RGO.

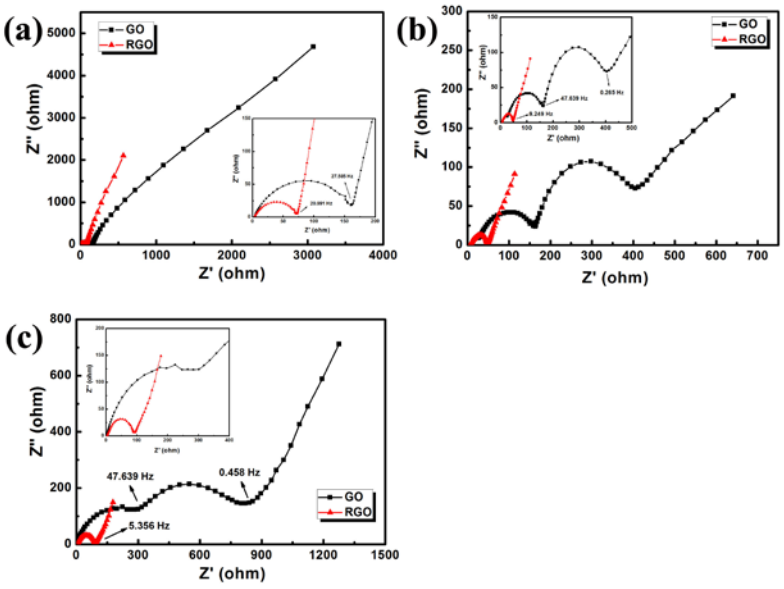

Fig. S8 Nyquist plots of GO and RGO at different cell states: (a) fresh cells, (b) 5^{th}-discharge and (c) 6^{th}-charge in the frequency range of 10^5 Hz to 0.01 Hz.

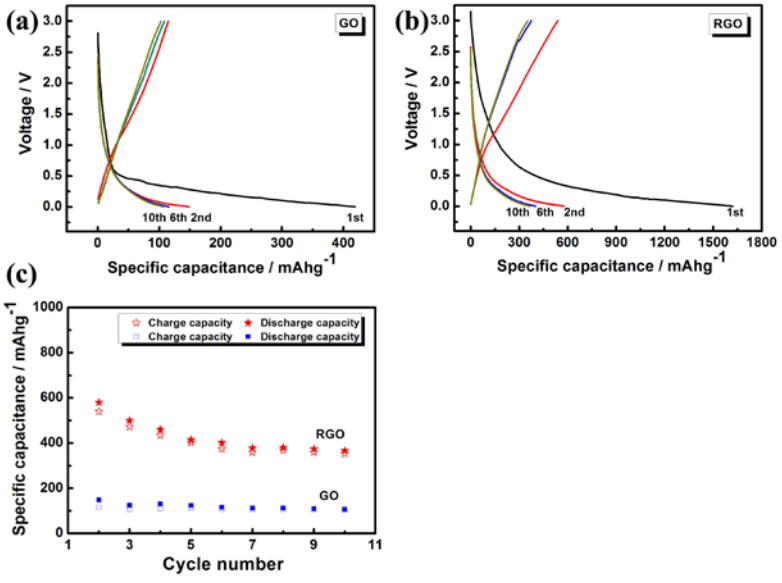

Fig. S9 (a, b) Galvanostatic charge/discharge profiles for selected cycles of GO and RGO at the current density of 40 mA g^{-1} with the potential window from 3.0 V to 0.001V, (c) Cycling performance of GO and RGO at 40 mA g^{-1}.

Electronic Supplementary Material (ESI) for Journal of Materials Chemistry A
This journal is (c) The Royal Society of Chemistry 2013

1. A. Gupta, G. Chen, P. Joshi, S. Tadigadapa and P. C. Eklud, *Nano Lett.*, 2006, **6**, 2667.

2. V. Singh, D. Joung, L. Zhai, S. Das, S. Khondaker and S. Seal, *Prog. Mater. Sci.*, 2011, **56**, 1178.

3. M. Ishii and M. Nakahira, *Solid State Commun.*, 1972, **11**, 209.